

# **The Bluefors Dilution Refrigerator as an Integrated Quantum Measurement System**

April 20, 2021

Russell Lake and Slawomir Simbierowicz  
Bluefors Quantum Team, Bluefors Oy,  
Arinatie 10, 00370 Helsinki, Finland

Philip Krantz  
Quantum Engineering Solutions, Keysight Technologies,  
1400 Fountaingrove Parkway, Santa Rosa, CA 95403-1738 USA

Farid Hassani and Johannes Fink  
Institute of Science and Technology Austria, Klosterneuburg 3400, Austria

# Table of Contents

1	Context .....	1
2	Application .....	1
3	Systems integration .....	1
3.1	Keysight qubit control solution.....	1
3.2	Bluefors dilution refrigerator .....	2
3.3	Quantum device.....	3
3.4	Wiring for quantum measurements .....	3
4	Experimental workflow .....	5
5	Measurement example.....	6
6	Conclusion .....	6
7	References .....	7

# Table of Figures

Figure 1: Bluefors LD250 cryostat with microwave wiring in an ISO KF-40 flange .....	2
Figure 2: Wiring schematic for the qubit integration experiment, minimum working example .....	4
Figure 3: a) Measurement of energy relaxation time, and b) histogram of results.....	6
Figure 4: Ramsey-fringes for varying qubit-drive detuning, as a function of time duration between the two $\pi/2$ pulses.....	6

# 1 Context

Measurements of quantum devices at millikelvin temperatures take on new importance today because of immediate applications in quantum simulations (Georgescu, Ashhab, & Nori, 2014), quantum sensing (Degen, Reinhard, & Cappellaro, 2017), and the world-wide race to build a fault tolerant quantum computer (Kjaergaard, et al., 2020). Scientists and engineers require integrated measurement systems to perform fast, and accurate characterization of quantum devices. The main measurement challenges are that devices require detection of very weak microwave signals and are exquisitely sensitive to environmental factors. Bluefors systems are often used as a platform for quantum devices as evidenced by more than 200 references (as of March 2021) to the Bluefors system in technical literature that focuses on quantum measurements or qubits.

This application note reports a decisive step towards demonstrating a "turn-key" integrated quantum measurement system that requires a vastly reduced number of steps required by the end-user to begin a quantum measurement. This advance is enabled by the integration of a PXI-based quantum measurement system from Keysight Quantum Engineering Solutions (QES) and the Labber instrument control software.

## 2 Application

The purpose of this application note is to demonstrate a working example of a superconducting qubit measurement in a Bluefors cryostat using the Keysight quantum control hardware. Our motivation is twofold. First, we provide pre-qualification data that the Bluefors cryostat, including filtering and wiring, can support long-lived qubits. Second, we demonstrate that the Keysight system (controlled using Labber) provides a straightforward solution to perform these characterization measurements. This document is intended as a brief guide for starting an experimental platform for testing superconducting qubits. The setup described here is an immediate jumping off point for a suite of applications including testing quantum logical gates, quantum optics with microwaves, or even using the qubit itself as a sensitive probe of local electromagnetic fields. Qubit measurements rely on high performance of both the physical sample environment and the measurement electronics. An overview of the cryogenic system is shown in Figure 1, and an overview of the integration between the electronics and cryostat (including wiring details) is shown in Figure 2.

## 3 Systems integration

### 3.1 Keysight qubit control solution

The control and readout of the qubit state has been outlined in a previous Keysight application note "[Characterizing Superconducting Qubits](#)." The signal generation and data acquisition sub-components of the measurement system are contained within a PXI-based quantum engineering tool-kit from Keysight. All modules are controlled using an embedded controller ([M9037A](#)) that runs the Labber software.

The PXIe chassis includes an arbitrary waveform generator ([M3202A](#)), a local oscillator ([M9347A](#)), and a digitizer ([M3102A](#)). The PXI offers advanced backplane triggering features known as a hard virtual instrument (HVI). In the present example, upconversion for qubit control and downconversion for qubit readout are implemented with discrete IQ mixers outside of the PXI chassis.

Measurements and data acquisition are performed using "[Labber](#)" — a powerful, yet user-friendly software package for instrument control and lab automation — with a focus on quantum applications.

### 3.2 Bluefors dilution refrigerator

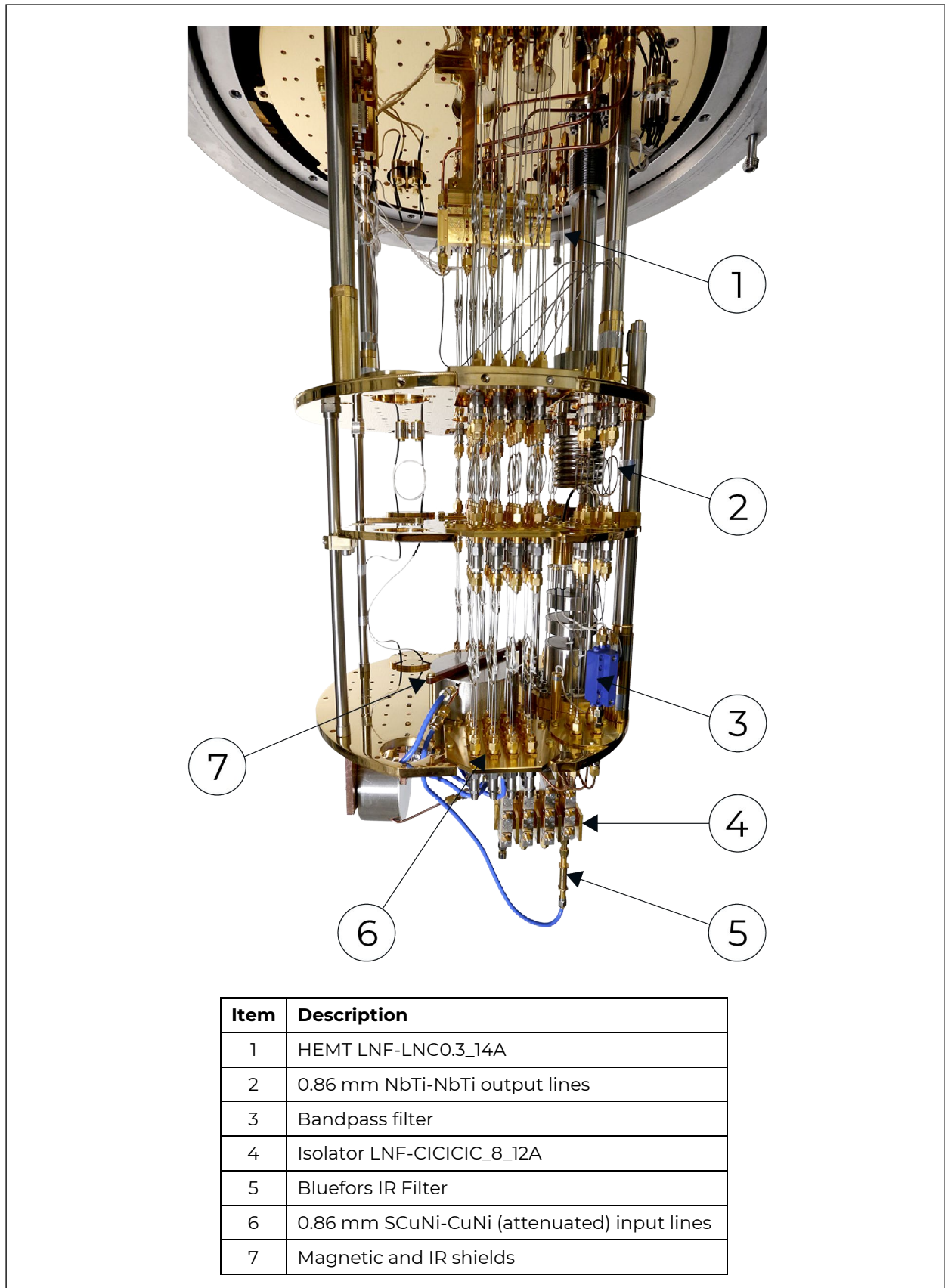


Figure 1: Bluefors LD250 cryostat with microwave wiring in an ISO KF-40 flange

We demonstrate integration between the Bluefors dilution refrigerator and the Keysight Quantum Control system by building an experimental setup at the Bluefors factory shown in Figure 1. We selected the most-sold dilution refrigerator measurement system at Bluefors: [LD250](#). The base temperature of the Mixing Chamber (MXC) Flange — where the quantum device is installed — is recorded to be 10 mK during the measurements. In this particular system, [36 microwave input and 4 microwave output lines](#) are pre-installed.

### 3.3 Quantum device

The [Fink Group](#) at IST-Austria designed and fabricated the quantum device used for this demonstration. In particular, we measure a single fixed-frequency transmon qubit through dispersive coupling to the TE<sub>101</sub> mode of the rectangular cavity used for readout. The cavity has a resonance frequency  $\omega_r/2\pi = 10.4$  GHz and the energy difference between the ground and excited state of the qubit corresponds to the frequency  $\omega_q/2\pi = 4.57$  GHz. With these parameters, the dispersive frequency shift is  $\chi/2\pi = 1$  MHz, and cavity decay rate is  $\kappa/2\pi = 250$  kHz. In addition to the large cavity-qubit detuning, the resonator is designed to be under-coupled from its input and output ports to further protect against Purcell decay.

### 3.4 Wiring for quantum measurements

For the example described here, one input line and one output line are used (Figure 2) to measure the cavity in transmission. The input lines are [Bluefors' coaxial wiring and installation sets](#) made from silver-plated cupronickel (SCuNi) with 0.86 mm outer diameter and added attenuation that is distributed along the line to protect the qubit from thermal radiation. The RF installation set (KF40) includes a hermetic feed-through at room temperature and 1x aluminum, 4x gold plated copper thermal anchoring flanges for the 50K, 4K, still, Cold plate and mixing chamber stages respectively. The flanges come with F/F bulkhead connectors for easy connection to the coaxial assemblies. At the mixing-chamber-stage the signal is further conditioned using low-pass filtering and the [Bluefors IR Filter](#) that is comprised of a 3-cm-long low-loss coaxial line that uses a microwave absorber as its dielectric. The filter absorbs and dissipates high-frequency noise that is far outside the measurement frequency band that would cause unwanted heating of the sample, or randomly change the qubit state. Insertion loss from the coaxial lines is approximately 10 dB at 10 GHz, with 61 dB of distributed added attenuation further blocks thermal radiation from each temperature stage (Yan, et al., 2018). Qubit control pulses are combined with the readout pulses at room temperature using a directional coupler. As shown in Figure 2, the readout line uses Bluefors' coaxial wiring options together with Bluefors' solution for Low Noise Factory amplifier and isolator integration. Between the Mixing Chamber Flange and the 4K Flange 0.86 mm NbTi-NbTi coaxial cables transmit the output signal. Between 4K and Room Temperature Flange, 2.19 mm SCuNi-CuNi cables are used. Additionally, the readout signal is filtered with low pass and band pass filtering, and the triple-stage isolators protect the qubit from High-Electron Mobility Transistor (HEMT) amplifier back-action.

The LD250 is equipped with a cylindrical gold-plated copper [radiation shield](#) that is attached at the still flange and surrounds the sample space. The 3D cavity is mounted within a dual-layer magnetic shield that includes a high-permeability material as its outer layer and an inner aluminum superconducting shield that expels ambient fields due to the Meissner effect. The inner shield has a rough, optically black coating that is also designed to absorb infrared (IR) radiation.

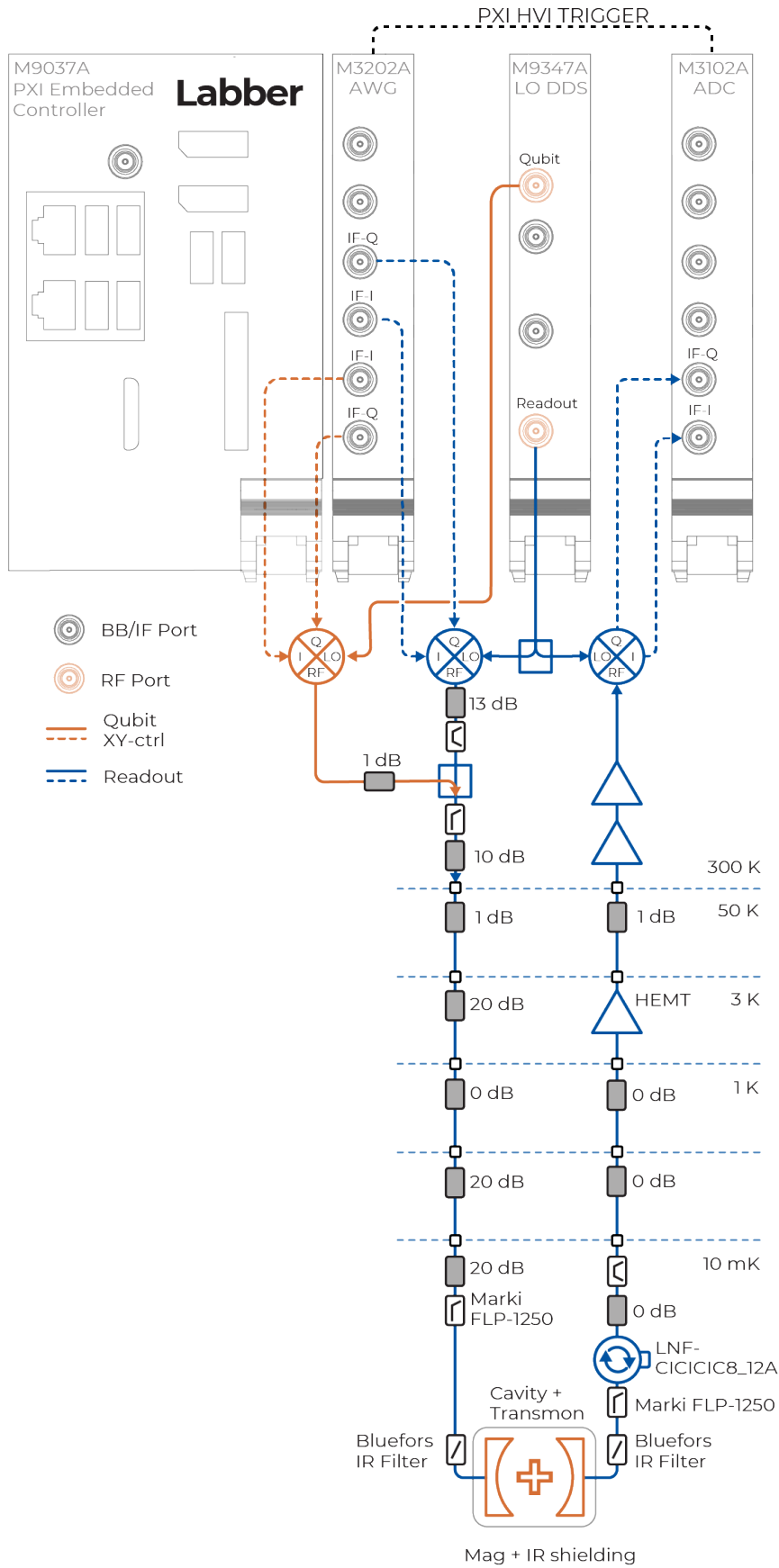


Figure 2: Wiring schematic for the qubit integration experiment, minimum working example

## 4 Experimental workflow

With the sub-systems of Section 3 in place, we are prepared to connect and probe the transmon qubit as summarized in the following steps.

1. Work with your Bluefors sales engineer to choose the optimal wiring configuration for your qubit measurement application: basic considerations for attenuator choices are described in the technical literature (Krinner, et al., 2019). Consider reflective bandpass filtering in your specific readout frequency band and absorptive infrared filtering such as the Bluefors IR Filter.
2. Install the packaged quantum device onto the base stage of the dilution refrigerator measurement system, and attach the blackbody and magnetic shielding. Make connections to input and output measurement lines. *Hint: most superconducting qubits do not require extra electrostatic discharge precautions.*
3. Power up the HEMT amplifiers at the 3 K stage, and the room-temperature microwave amplifiers. In practice, using low-noise amplifiers at both 3 K and 300 K, a total gain of 70 dB – 80 dB before down-conversion will be sufficient to measure qubit dynamics with ensemble averaging. A parametric amplifier at base temperature will further reduce the noise temperature (Simbierowicz, et al., 2021) to enable single-shot readout.
4. Characterize the device spectrum with continuous-wave microwave test equipment such as the [Keysight Precision Network Analyzer \(PNA\)](#). Program a frequency-dependent transmission sweep using the built-in Labber driver to find the resonance frequency of the readout cavity. Repeat the measurement at different "resonator probe" powers to observe the frequency shift caused by dispersive interaction between the qubit and resonator modes (Krantz, et al., 2019). The observed frequency shift provides a signature that the qubit is operational.
5. Connect to the LO DDS module, the Keysight PXI AWG module, and the Keysight Digitizer module to the dilution refrigerator measurement system, as shown in Figure 2. Add all of these modules to the Labber instrument server, along with the "Keysight PXI HVI Trigger" and the "Multi-Qubit Pulse Generator", which we will use for the pulse generation for qubit control and readout. See the Application Note "[Characterizing Superconducting Qubits](#)" for a detailed description of how to set up and configure Labber.
6. Next, the qubit transition frequency  $f_{01}$  can be found using qubit spectroscopy. To do this, we combine the resonator probe with the qubit drive by using a directional coupler. Since we want to investigate the coherence properties of the qubit, we need to move to the time-domain, using the Keysight PXI system. After re-scanning the readout resonator using the AWG/Digitizer setup, we choose a resonator probe power for which the resonator has not shifted due to the qubit and pick a readout frequency bias point<sup>1</sup>. We can now scan for the qubit frequency by sweeping the qubit probe, while monitoring the magnitude and phase response of the resonator.

## 5 Measurement example

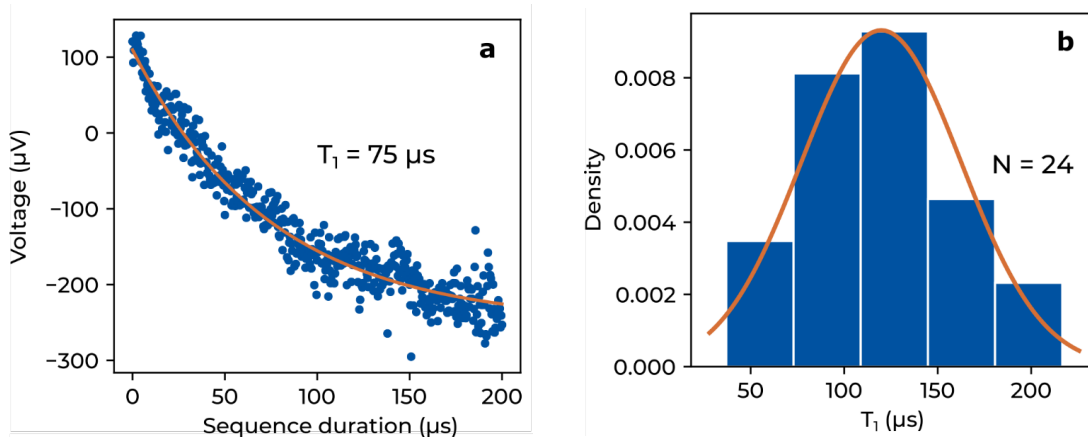


Figure 3: a) Measurement of energy relaxation time, and b) histogram of results

After initial spectroscopy experiments, and calibration of a  $\pi$ -pulse we briefly investigate the qubit dynamics using built-in applications and drivers in Labber. A key figure of merit for the qubit chip, and its environment is the energy-relaxation time  $T_1$ , i.e., the time constant for the exponential decay between the first excited state and the ground state. We vary the duration of the readout-delay between the applied  $\pi$ -pulse and the readout tone and plot the results in Figure 3. Without extensive optimization, we observe energy relaxation time is comparable with state-of-the-art for 3D transmons within the Bluefors factory (Kjaergaard, et al., 2020). In Figure 3 a) we show a single measurement of the energy relaxation time for our superconducting qubit and an exponential fit to the data. In Figure 3 b) we plot a histogram with  $N = 24$  repeated measurements. The orange line is a fitted normal distribution with a mean of  $120 \mu\text{s}$ .

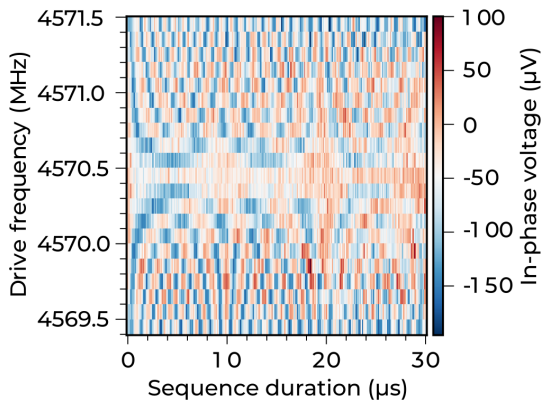


Figure 4: Ramsey-fringes for varying qubit-drive detuning, as a function of time duration between the two  $\pi/2$  pulses

In addition, we can perform a Ramsey experiment by preparing the qubit in a superposition state  $\frac{1}{\sqrt{2}}(|0\rangle + |1\rangle)$  using two consecutive  $\pi/2$  pulses, at a given detuning frequency from the qubit, with readout following immediately after the second pulse. Varying the time between pulses and the offset frequency creates an interference pattern as shown in Figure 4, demonstrating quantum coherence in the one-qubit system. In Figure 4, the color scale indicates the amplitude of average measured signal after the second  $\pi/2$  pulse, which is proportional to the ensemble average of the qubit polarization.

## 6 Conclusion

In conclusion, we demonstrate a working example of characterizing a single superconducting qubit in the Bluefors LD250, using the PXI-based Keysight quantum control system. The measured qubit coherence suggests that thermalization, shielding, and signal filtering are sufficient to observe expected

performance for a 3D transmon. We attribute this relatively long energy-relaxation time to both careful design and fabrication of the qubit sample, as well as the cryogenic environment. In particular, our configuration includes low-loss Bluefors IR Filters that are placed at both the input and output of the sample ports, that are designed to absorb and dissipate high frequency radiation that can otherwise lead to spurious quasiparticle excitation on the qubit chip. Factory-installed coaxial wiring, IR filtering, and low-noise amplification at the 4K Flange guarantee sufficient signal-to-noise ratio for operation with the Keysight hardware. Finally, using the Labber instrument control software, we demonstrate a turn-key quantum control solution for quantum applications.

## 7 References

- Degen, C. L., Reinhard, F., & Cappellaro, P. (2017). Quantum Sensing. *Reviews of Modern Physics*, 89, 035002. doi:10.1103/RevModPhys.89.035002
- Georgescu, I. M., Ashhab, S., & Nori, F. (2014). Quantum simulation. *Reviews of Modern Physics*, 86, 153. doi:10.1103/RevModPhys.86.153
- Kjaergaard, M., Schwartz, M. E., Braümmüller, J., Krantz, P., Wang, J. I.-J., Gustavsson, S., & Oliver, W. D. (2020). Superconducting Qubits: Current State of Play. *Annual Review of Condensed Matter Physics*, 11(1), 369-395. doi:10.1146/annurev-conmatphys-031119-050605
- Krantz, P., Kjaergaard, M., Yan, F., Orlando, T. P., Gustavsson, S., & Oliver, W. D. (2019). A quantum engineer's guide to superconducting qubits. *Applied Physics Reviews*, 6, 021318. doi:10.1063/1.5089550
- Krinner, S., Storz, S., Kurpiers, P., Magnard, P., Heinsoo, J., Keller, R., . . . Wallraff, A. (2019). Engineering cryogenic setups for 100-qubit scale superconducting circuit systems. *EPJ Quantum Technol.*, 6, 2. doi:10.1140/epjqt/s40507-019-0072-0
- Simbierowicz, S., Vesterinen, V., Milem, J., Lintunen, A., Oksanen, M., Roschier, L., . . . Lake, R. E. (2021). Characterizing cryogenic amplifiers with a matched temperature-variable noise source. *Review of Scientific Instruments*, 92, 034708. doi:10.1063/5.0028951
- Yan, F., Campbell, D., Krantz, P., Kjaergaard, M., Kim, D., Yoder, J. L., . . . Oliver, W. D. (2018). Distinguishing Coherent and Thermal Photon Noise in a Circuit Quantum Electrodynamical System. *Physical Review Letters*, 120, 260504. doi:10.1103/PhysRevLett.120.260504

---

<sup>i</sup> When picking the bias point, some consideration to the expected dispersive frequency shift need to be taken into account.